Preprints of the 19th World Congress
The International Federation of Automatic Control
Cape Town, South Africa. August 24-29, 2014

Lyapunov-based Adaptive Regulation of Limit Cycle Oscillations in Aircraft Wings Using Synthetic Jet Actuators ⋆

Natalie Ramos Pedroza * **William MacKunis** *
Barrett F. Guenthoer ** **Vladimir V. Golubev** **
J. Willard Curtis ***

* *Department of Physical Sciences, Embry-Riddle Aeronautical University, Daytona Beach, FL 32114 USA (email: ramosa66@my.erau.edu, mackuniw@erau.edu)*
** *Department of Aerospace Engineering, Embry-Riddle Aeronautical University, Daytona Beach, FL 32114 USA (email: guent80c@my.erau.edu, golubd1b@erau.edu)*
*** *Air Force Research Laboratory Munitions Directorate, Eglin Air Force Base, FL 32542 USA (email: jess.curtis@eglin.af.mil)*

Abstract: In this paper, a SJA-based nonlinear adaptive controller is developed, which is capable of completely suppressing LCO in UAV systems with uncertain actuator dynamics. Specifically, the control law compensates for uncertainty in an input gain matrix, which results from the unknown airflow dynamics generated by the SJA. Challenges in the control design include compensation for input-multiplicative parametric uncertainty in the actuator dynamic model. This difficulty was handled via innovative algebraic manipulation in the error system development, along with a Lyapunov-based adaptive law. A rigorous Lyapunov-based stability analysis is utilized to prove asymptotic plunging regulation, considering a detailed dynamic model of the pitching and plunging dynamics; and numerical simulation results are provided to demonstrate that simultaneous pitching and plunging suppression is achieved using the proposed control law.

Keywords: Adaptive system and control, nonlinear adaptive control, Lyapunov stability analysis, limit cycle oscillations, synthetic jet actuators

1. INTRODUCTION

There has recently been a surge of interest in the design and application of unmanned aerial vehicles (UAV). These UAVs can be used in numerous civilian applications, such as urban reconnaissance, package delivery, and area mapping; UAVs are utilized in various military applications as well. One of the biggest challenges involved in the autonomous operation of UAVs is in the design of flight tracking controllers for UAVs operating in uncertain and possibly adverse conditions. In particular, suppression of limit cycle oscillations (LCO) (or flutter) is an important concern in UAV tracking control design. This is especially true for applications involving smaller, lightweight UAV systems, where the aircraft wings are more susceptible to LCO. These engineering challenges necessitate the utilization of UAV flight controllers, which achieve accurate flight tracking in the presence of dynamic uncertainty while simultaneously suppressing LCO. Moreover, as practical considerations motivate the implementation of smaller UAVs, there is a growing need for UAV flight control designs that do not require heavy mechanical deflection surfaces.

LCO refer to "flutter" behavior in UAV wings that manifest themselves as constant-amplitude oscillations (O'Donnell et al. (2007)), which result from nonlinearities inherent in the aeroelastic dynamics of the UAV system (Satak et al. (2012)). Due to these behaviors, the LCO would surpass the limiting safe flight boundaries of an aircraft (Rubillo et al. (2005)) and could potentially lead to structural damage and catastrophes. Control applications for LCO suppression are often developed (e.g., see Frampton and Clark (2000); Strganac et al. (2000); Platanitis and Strganac (2004)) using mechanical deflection surfaces (e.g. flaps, ailerons, rudders, and elevators). However, when dealing with small UAVs, practical engineering considerations and physical constraints can preclude the addition of the large, heavy moving parts that are required for the installation of deflection surfaces. To address this challenge, the use of synthetic jet actuators (SJA) in UAV flight control systems is becoming popular as a practical alternative to mechanical deflection surfaces.

The design and application of SJA has recently increased by virtue of their capability to achieve momentum transfer with zero-net mass-flux. This beneficial feature eliminates

⋆ This research is supported in part by a grant from the American Society for Engineering Education Air Force Summer Faculty Fellowship Program.

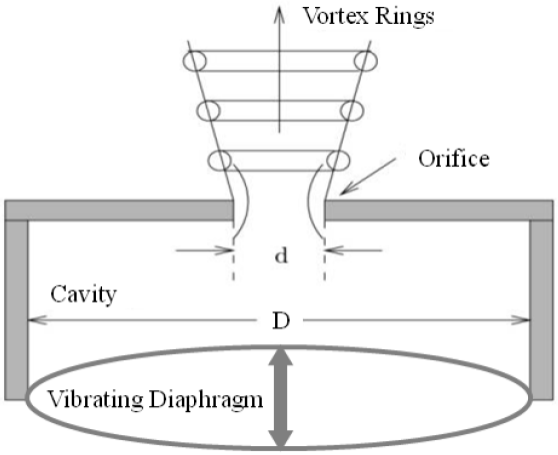

Fig. 1. Schematic layout of a Synthetic Jet Actuator.

the need for an external fuel supply, since the working substance is simply the gas (i.e., air) that is already present in the environment of operation (Mackunis et al. (2013)). This makes SJA an attractive option in UAV applications, because of the significant reduction in size of the required equipment. The SJA synthesize the jet flow through the alternating suction and ejection of fluid through an aperture, which is produced via pressure oscillations in a cavity (Jee et al. (2013)) as shown in Fig. 1. The pressure oscillations can be generated using various methods, including pistons in the SJA orifices (Rubillo et al. (2005)) or piezoelectric diaphragms (Deb et al. (2005b); Mackunis et al. (2013)). SJA can achieve boundary-layer flow control near the surface of a UAV wing (Milanese et al. (2008)), since they can provide instant actuation, unlike conventional mechanical control surfaces. In addition, SJA can expand the usable range of angle of attack, resulting in improved UAV maneuverability (Amitay et al. (2001)).

Recently developed nonlinear control methods using SJA typically utilize neural networks and/or complex fluid dynamics computations in the feedback loop (e.g., see Tchieu et al. (2008); Mondschein et al. (2011); Deb et al. (2005b,a, 2006, 2007, 2008); Liu et al. (2006); Singhal et al. (2009); Tao (1996); Jee et al. (2009); Milanese et al. (2008)). While such approaches have been shown to yield good SJA-based control performance, they can require increased computational resources, which might not be available in small UAV applications. Adaptive control approaches have been applied to linear time-invariant (LTI) dynamic models to compensate for SJA nonlinearities and external disturbances (Mondschein et al. (2011)). Adaptive inverse control schemes are another popularly utilized method to compensate for the actuator nonlinearity inherent in SJA (Deb et al. (2005b,a, 2006, 2007, 2008)). A robust tracking control method is proposed in (Mackunis et al. (2013)), which builds on results similar to (Deb et al. (2005b,a, 2006, 2007, 2008)), to compensate for the SJA nonlinearity at a reduced computational cost. The aforementioned approaches have been shown to achieve good flight tracking performance using SJA; however, nonlinear control approaches have not as often been applied to SJA-based LCO suppression.

In this paper, a SJA-based nonlinear adaptive controller is developed, which is capable of completely suppressing LCO in UAV systems with uncertain dynamics. Specifically, the control law compensates for uncertainty in an input gain matrix, which results from uncertainty in the airflow dynamics generated by the SJA. Challenges in the control design include input-multiplicative parametric uncertainty in the dynamic model. This difficulty was handled via innovative algebraic manipulation in the error system development, along with a Lyapunov-based adaptive law. A rigorous Lyapunov-based stability analysis is utilized to prove asymptotic plunging regulation, considering a detailed dynamic model of the pitching and plunging dynamics; and numerical simulation results are provided to demonstrate simultaneous pitching and plunging suppression using the proposed control law.

2. DYNAMIC MODEL AND PROPERTIES

The equation describing LCO in an airfoil approximated as a 2-dimensional thin plate can be expressed as

$$M_s\ddot{p} + C_s\dot{p} + F(p)p = \begin{bmatrix} -Lift \\ Moment \end{bmatrix} \tag{1}$$

where the coefficients $M_s, C_s \in \mathbb{R}^{2\times 2}$ denote the structural mass and damping matrices, $F(p) \in \mathbb{R}^{2\times 2}$ is a nonlinear stiffness matrix, and $p(t) \in \mathbb{R}^2$ denotes the state vector. In (1), $p(t)$ is explicitly defined as

$$p = \begin{bmatrix} h \\ \alpha \end{bmatrix} \tag{2}$$

where $h(t)$, $\alpha(t) \in \mathbb{R}$ denote the plunging [meters] and pitching [radians] displacements describing the LCO effects. Also in (1), the structural linear mass matrix M_s is defined as (Dreyer (2008))

$$M_s = \begin{bmatrix} m & S_\alpha \\ S_\alpha & I_\alpha \end{bmatrix} \tag{3}$$

where the parameters S_α, $I_\alpha \in \mathbb{R}$ are the static moment and moment of inertia, respectively. The structural linear damping matrix is described as

$$C_s = 2\begin{bmatrix} \zeta_h\sqrt{k_h m} & 0 \\ 0 & \zeta_a\sqrt{k_\alpha I_\alpha} \end{bmatrix} \tag{4}$$

where the parameters ζ_h, $\zeta_\alpha \in \mathbb{R}$ are the damping logarithmic decrements for plunging and pitching, and $m \in \mathbb{R}$ is the mass of the wing, or in this case, a flat plate. The nonlinear stiffness matrix utilized in this study is

$$F(p) = \begin{bmatrix} k_h & 0 \\ 0 & k_\alpha + k_{\alpha^3}\alpha^2 \end{bmatrix} \tag{5}$$

where $k_\alpha, k_{\alpha^3} \in \mathbb{R}$ denote structural resistances to pitching (linear and nonlinear) and $k_h \in \mathbb{R}$ is the structural resistance to plunging. The right hand side of (1) is given by (Dreyer (2008); Milanese et al. (2008))

$$\begin{bmatrix} -Lift \\ Moment \end{bmatrix} = \begin{bmatrix} -(L + L_{v_j}) \\ (M + M_{v_j}) \end{bmatrix} \tag{6}$$
$$= M_a\ddot{p} + C_a\dot{p} + K_a p + L_\eta\eta + B_1 v_j + B_2\dot{v}_j$$

where $L_{v_j}(t), M_{v_j}(t) \in \mathbb{R}$ denote the control contributions due to the SJA, and L, $M \in \mathbb{R}$ are the aerodynamic lift and moment due to the 2 degrees-of-freedom motions (Milanese et al. (2008)). The $\eta \in \mathbb{R}^2$ are the aerodynamic state vectors that relates the moment and lift to the modes.

Terms $v_j(t) \in \mathbb{R}$ and $\dot{v}_j(t) \in \mathbb{R}$ are the SJA control input (air) velocity and acceleration, respectively. The constant vectors B_1, $B_2 \in \mathbb{R}^{2\times 2}$ are defined

$$B_1 = \begin{bmatrix} -U\rho b I_1 \\ U\rho b^2 I_2 + aU\rho b^2 I_1 \end{bmatrix} \tag{7}$$

$$B_2 = \begin{bmatrix} -\rho b^2 I_2 \\ -\frac{1}{2}\rho b^3 I_3 + a\rho b^3 I_2 \end{bmatrix} \tag{8}$$

where the constant $\rho \in \mathbb{R}$ denotes the density of air, and $U \in \mathbb{R}$ is the mean free-stream velocity. The parameters a, $b \in \mathbb{R}$ denote the relative location of the rotational axis from the midchord and the semi-chord, respectively. The functions I_1, I_2, $I_3 \in \mathbb{R}$ (Milanese et al. (2008)) are linked to the control force distribution, and they are explicitly defined as

$$I_1 = \int_{\Theta_1}^{\Theta_2} sin(\Theta) tan^{-1}\left(\frac{\Theta}{2}\right) d\Theta \tag{9}$$

$$I_2 = \frac{1}{2}\left[\Theta_2 - \Theta_1 + \frac{1}{2}sin(2\Theta_1) - \frac{1}{2}sin(2\Theta_2)\right] \tag{10}$$

$$I_3 = \frac{1}{3}\left[sin^3(\Theta_2) - sin^3(\Theta_1)\right]. \tag{11}$$

The parameters Θ_1 and Θ_2 are the optimal synthetic jet locations (Milanese et al. (2008)). The aerodynamic matrices M_a, C_a, $K_a \in \mathbb{R}^{2\times 2}$ are described as

$$M_a = \pi\rho b^2 \begin{bmatrix} -1 & ba \\ ba & -b^2\left(\frac{1}{8} - a^2\right) \end{bmatrix} \tag{12}$$

$$C_a = \pi\rho b^2 \begin{bmatrix} 0 & -U \\ 0 & -Ub\left(\frac{1}{2} - a\right) \end{bmatrix} \tag{13}$$

$$+2\pi\rho Ub\phi(0) \begin{bmatrix} -1 & -b\left(\frac{1}{2} - a\right) \\ b\left(\frac{1}{2} + a\right) & b^2\left(\frac{1}{2} + a\right)\left(\frac{1}{2} - a\right) \end{bmatrix}$$

$$K_a = 2\pi\rho Ub\phi(0) \begin{bmatrix} 0 & -U \\ 0 & b\left(\frac{1}{2} + a\right) U \end{bmatrix} \tag{14}$$

$$L_\eta = 2\pi\rho Ub \begin{bmatrix} a_1 b_1 & a_2 b_2 \\ -b\left(\frac{1}{2} + a\right) a_1 b_1 & -b\left(\frac{1}{2} + a\right) a_2 b_2 \end{bmatrix} \tag{15}$$

where $\phi(0)$ is the Wagner solution function at 0, and the parameters a_1, b_1, a_2, $b_2 \in \mathbb{R}$ are the Wagner coefficients.

The aerodynamic state variables are governed by (Dreyer (2008))

$$\dot{\eta} = C_\eta \dot{p} + K_\eta p + S_\eta \eta \tag{16}$$

The aerodynamic state matrices in (16), C_η, K_η, $S_a \in \mathbb{R}^{2\times 2}$, are explicitly defined as

$$C_\eta = \frac{U}{b} \begin{bmatrix} -1 & -b\left(\frac{1}{2} - a\right) \\ -1 & -b\left(\frac{1}{2} - a\right) \end{bmatrix} \tag{17}$$

$$K_\eta = \frac{U}{b} \begin{bmatrix} 0 & -U \\ 0 & -U \end{bmatrix} \tag{18}$$

$$S_\eta = \frac{U}{b} \begin{bmatrix} -b_1 & 0 \\ 0 & -b_2 \end{bmatrix}. \tag{19}$$

By rearranging (1) and (6) and solving for $\ddot{p}(t)$, the equation becomes

$$\ddot{p} = -\frac{C}{M}\dot{p} - \frac{K}{M}p + \frac{L_\eta}{M}\eta + \frac{B_1}{M}v_j + \frac{B_2}{M}\dot{v}_j \tag{20}$$

where $C = C_s - C_a$, $K = F(p) - K_a$, and $M = M_s - M_a$.

The dynamic equation in (20) can be expressed in state form as

$$\dot{x} = A(x)x + \hat{B}_1 v_j + \hat{B}_2 \dot{v}_j \tag{21}$$

where $\dot{v}_j(t)$ denotes the control input, $x(t) \in \mathbb{R}^6$ is the state vector, $A(x) \in \mathbb{R}^{6\times 6}$ is the state matrix (nonlinear), and $\hat{B}_1$, $\hat{B}_2 \in \mathbb{R}^{6\times 1}$ are defined as

$$\hat{B}_1 = \begin{bmatrix} 0 \\ 0 \\ M^{-1}B_1 \\ 0 \\ 0 \end{bmatrix} \tag{22}$$

$$\hat{B}_2 = \begin{bmatrix} 0 \\ 0 \\ M^{-1}B_2 \\ 0 \\ 0 \end{bmatrix} \tag{23}$$

where B_1 and B_2 are the control input gain terms, which only directly affect $\ddot{h}(t)$ and $\ddot{\alpha}(t)$. By making the definitions $x_1 = h$, $x_2 = \alpha$, $x_3 = \dot{h}$, $x_4 = \dot{\alpha}$, $x_5 = \eta_1$, and $x_6 = \eta_2$; and defining $\dot{x}_1 = x_3$, $\dot{x}_2 = x_4$, $\dot{x}_3 = \ddot{h}$, $\dot{x}_4 = \ddot{\alpha}$, $\dot{x}_5 = \dot{\eta}_1$, and $\dot{x}_6 = \dot{\eta}_2$, the state vector and its derivative can be expressed as

$$x \triangleq \left[x_1 \; x_2 \; x_3 \; x_4 \; x_5 \; x_6\right]^T, \tag{24}$$

$$\dot{x} \triangleq \left[\dot{x_1} \; \dot{x_2} \; \dot{x_3} \; \dot{x_4} \; \dot{x_5} \; \dot{x_6}\right]^T. \tag{25}$$

After expressing (20) in state space form similar to (21) and solving for the corresponding coefficients, the $A(x)$ state matrix can be explicitly obtained.

3. CONTROL DEVELOPMENT

The objective is to design the scalar control signal $\dot{v}_j(t)$ to regulate the plunge dynamics (i.e., $h(t)$) to zero. The plunging dynamics can be expressed as

$$\ddot{h} = -c_1\dot{h} - c_2\dot{\alpha} - c_3 h - c_4\alpha + c_5\eta_1 + c_6\eta_1 + b_1 v_j + b_2\dot{v}_j, \tag{26}$$

where c_1, c_2, c_3, c_4, c_5, $c_6 \in \mathbb{R}$ are the coefficients related to $A(x)$. The coefficients b_1 and b_2 are unknown constant control input gain terms, which relate the SJA dynamics to the plunging dynamics. The expression in (27) can be rewritten as

$$\ddot{h} = g(h, \alpha, \eta) + b_1 v_j + b_2 \dot{v}_j \tag{27}$$

where $g(h, \alpha, \eta)$ satisfies inequality

$$\|g(h, \alpha, \eta)\| \leq \rho_0 \|z\| \tag{28}$$

where $\rho_0 \in \mathbb{R}^+$ is a known bounding constant, and $z(t) \in \mathbb{R}^{2n}$ is defined as

$$z \triangleq \left[e \; r\right]^T. \tag{29}$$

To facilitate the subsequent control development and stability analysis, a tracking error $e(t)$ and an auxiliary tracking error variable $r(t)$ are defined as

$$e = h - h_d = h - 0 \tag{30}$$

$$r = \dot{e} + \alpha_g e = \dot{h} + \alpha_g h \tag{31}$$

where $\alpha_g > 0 \in \mathbb{R}$ is a user defined control gain, and the desired plunging state $h_d = 0$ for the plunging suppression objective. To facilitate the following analysis, the time derivative of (31) is calculated as

$$\dot{r} = \ddot{h} + \alpha_g \dot{h}. \tag{32}$$

After substituting for $\ddot{h}(t)$ in (27) and using (32) the following is obtained:

$$\begin{aligned} \ddot{h} &= g(h, \alpha, \eta) + Y_1 \theta_1 + \Omega \dot{v}_j \\ \dot{r} &= g(h, \alpha, \eta) + Y_1 \theta_1 + \Omega \dot{v}_j + \alpha_g \dot{h} \end{aligned} \tag{33}$$

where $Y_1(v_j) \in \mathbb{R}$ is measurable regressor, and $\theta_1 \in \mathbb{R}$ is an unknown constant defined via the parameterization

$$Y_1 \theta_1 \triangleq b_1 v_j. \tag{34}$$

In Equation (33), $\Omega(b_2) \in \mathbb{R}$ denotes an uncertain constant auxiliary term defined via the parameterization

$$\Omega \dot{v}_j \triangleq b_2 \dot{v}_j. \tag{35}$$

The expression in (35) can be reparameterized in terms of a known regressor $Y_2(\dot{v}_j) \in \mathbb{R}$ and an unknown constant $\theta_2 \in \mathbb{R}$ as

$$\Omega \dot{v}_j \triangleq Y_2 \theta_2. \tag{36}$$

To address the issue of the control input $\dot{v}_j(t)$ being multiplied by the uncertain term Ω as in (33), an estimate of the uncertainty $\hat{\Omega}(t) \in \mathbb{R}$ is defined via

$$\hat{\Omega} \dot{v}_j \triangleq Y_2 \hat{\theta}_2 \tag{37}$$

where $\hat{\theta}_2(t) \in \mathbb{R}$ is a subsequently designed estimate of the parametric uncertainty in $\Omega(b_2)$. Based on (36) and (37), (33) can be expressed as

$$\dot{r} = g(h, \alpha, \eta) + \alpha_g \dot{h} + Y_1 \theta_1 + \hat{\Omega} \dot{v}_j + Y_2 \tilde{\theta}_2 \tag{38}$$

where the parameter estimate mismatch $\tilde{\theta}_2(t) \in \mathbb{R}$ is defined as

$$\tilde{\theta}_2 \triangleq \theta_2 - \hat{\theta}_2. \tag{39}$$

Based on the open-loop error dynamics in (38), the control input is designed as

$$\dot{v}_j = \hat{\Omega}^{-1} \left(-(k_s + 1) r - Y_1 \hat{\theta}_1 - h \right) \tag{40}$$

Remark 1. To ensure that no singularities are encountered during closed-loop controller operation, the time-varying adaptive estimates in $\hat{\Omega}$ are generated using a standard projection algorithm, which is used to guarantee that $\hat{\Omega} \neq 0$.

Using (40) and the open loop dynamics in (38), the closed loop system is obtained as

$$\dot{r} = \tilde{N} + Y_1 \tilde{\theta}_1 + Y_2 \tilde{\theta}_2 - (k_s + 1) r - h, \tag{41}$$

where the parameter estimate mismatch $\tilde{\theta}_1(t) \in \mathbb{R}$ is defined as

$$\tilde{\theta}_1 \triangleq \theta_1 - \hat{\theta}_1. \tag{42}$$

In (41), the unknown, unmeasurable auxiliary function $\tilde{N}(t) \in \mathbb{R}$ is defined as

$$\tilde{N} \triangleq g(h, \alpha, \eta) + \alpha_g \dot{h}. \tag{43}$$

The auxiliary term $\tilde{N}(t)$ satisfies the inequality

$$\|\tilde{N}\| \leq \rho_0 \|z\|. \tag{44}$$

Based on (41) and the following stability analysis, the adaptive estimates $\hat{\theta}_1(t)$ and $\hat{\theta}_2(t)$ are generated online according to the following adaptive update laws:

$$\dot{\hat{\theta}}_1 = \gamma_1 proj\left(Y_1^T r\right), \qquad \dot{\hat{\theta}}_2 = -\gamma_2 proj\left(Y_2^T r\right) \tag{45}$$

where $\gamma_1, \gamma_2 \in \mathbb{R}$ are positive constant adaptation gains. The function $proj(\cdot)$ is a normal projection algorithm, which ensures that the following inequalities are satisfied (Zergeroglu et al. (2000); Dixon (2007))

$$\underline{\theta}_1 \leq \hat{\theta}_1 \leq \bar{\theta}_1 \tag{46}$$

$$\underline{\theta}_2 \leq \hat{\theta}_1 \leq \bar{\theta}_2 \tag{47}$$

where $\underline{\theta}_1, \bar{\theta}_1, \underline{\theta}_2, \bar{\theta}_2 \in \mathbb{R}$ denote known lower and upper bounds on $\hat{\theta}_1(t)$ and $\hat{\theta}_2(t)$, respectively.

3.1 Stability Analysis

Theorem 1. The adaptive controller in (40) ensures asymptotic regulation of the plunging displacement in the sense that

$$|h(t)| \to 0 \quad \text{as} \quad t \to \infty. \tag{48}$$

Proof. Let $V\left(r, h, \tilde{\theta}_1, \tilde{\theta}_2\right)$ denote the following radially unbounded positive definite Lyapunov function:

$$V = \frac{1}{2} h^2 + \frac{1}{2} r^2 + \frac{\gamma_1^{-1}}{2} \tilde{\theta}_1^2 + \frac{\gamma_2^{-1}}{2} \tilde{\theta}_2^2. \tag{49}$$

After taking the time derivative (49) and substituting (41) and (31), $\dot{V}(t)$ is obtained as

$$\begin{aligned} \dot{V} = r \left(Y_1 \tilde{\theta}_1 + Y_2 \tilde{\theta}_2 - (k_s + 1) r - h + \tilde{N} \right) \\ + h(r - \alpha_g h) - \gamma_1^{-1} \tilde{\theta}_1 \dot{\hat{\theta}}_1 - \gamma_2^{-1} \tilde{\theta}_2 \dot{\hat{\theta}}_2. \end{aligned} \tag{50}$$

After using the adaptive laws in (45), the expression in (50) can be used to upper bound $V(t)$ as

$$\dot{V} \leq -\alpha_g \|h\|^2 + \left[\rho_z \|r\| \|z\| - \lambda_{\min}(k_s) \|r\|^2 \right] \tag{51}$$

After completing the squares for the bracketed term in (51), the upper bound on $\dot{V}(t)$ can be expressed as

$$\dot{V} \leq -\lambda \|z\|^2 + \frac{\rho_z^2 \|z\|^2}{4 \lambda_{\min}(k_s)} \tag{52}$$

where $\lambda \triangleq \min\{\alpha_g, 1\}$ and $z(t)$ is defined in (29). The expressions in (49) and (52) can be used to conclude that $h(t) \in \mathcal{L}_\infty$ and $r(t) \in \mathcal{L}_\infty$. Since, $h(t)$, $r(t) \in \mathcal{L}_\infty$, $\dot{h}(t) \in \mathcal{L}_\infty$ from (31). Given that $\dot{h}(t) \in \mathcal{L}_\infty$, $h(t)$ is uniformly continuous. The expressions in (52) and (49) can be used to prove that $h(t) \in \mathcal{L}_\infty \cap \mathcal{L}_2$. Barbalat's lemma (Khalil (2002)) can now be invoked to prove that $\|h(t)\| \to 0$ as $t \to \infty$. Further, given that $V(t)$ in (49) is radially unbounded, convergence of $h(t)$ is guaranteed, regardless of initial conditions - a global result. ■

4. SIMULATION RESULTS

A numerical simulation was created to demonstrate the performance of the control law developed in (40). The simulation is based on the dynamic model given in (1) and (16). The dynamic parameters utilized in the simulation are summarized in Table 1 and were obtained from Dreyer (2008).

The parameters $\Theta_1 = 1.6$ and $\Theta_2 = 1.7$ are the synthetic jet locations that result in a lift overshoot reduction of 21%

Table 1. Constant parameters

$\rho = 1.225 \frac{kg}{m^3}$	$a = -0.24$	$U = 18 \frac{m}{s}$
$m = 2.55kg$	$b = 0.11m$	$v = 18 \frac{m}{s}$
$S_\alpha = 10.4 \times 10^{-3} kg \cdot m$	$a_1 = 0.1650$	$a_2 = 0.0455$
$I_\alpha = 2.51 \times 10^{-3} kg \cdot m$	$b_1 = 0.3350$	$b_2 = 0.3000$
$k_h = 450 \frac{N}{m}$	$k_\alpha = 9.3 \frac{N}{m}$	$k_{\alpha^3} = 55 \frac{N}{m}$
$\zeta_h = 5.5 \times 10^{-3}$	$\zeta_\alpha = 1.8 \times 10^{-2}$	

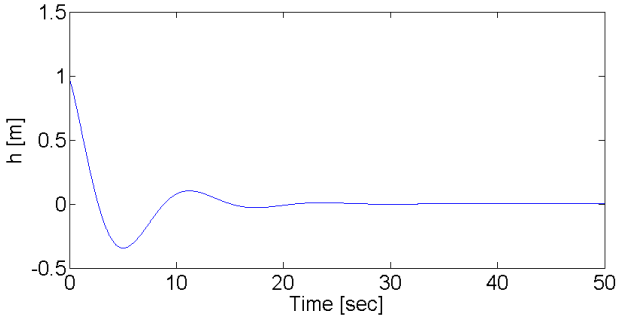

Fig. 2. Convergence of the tracking error for plunging, $h(t)$ in $[m]$.

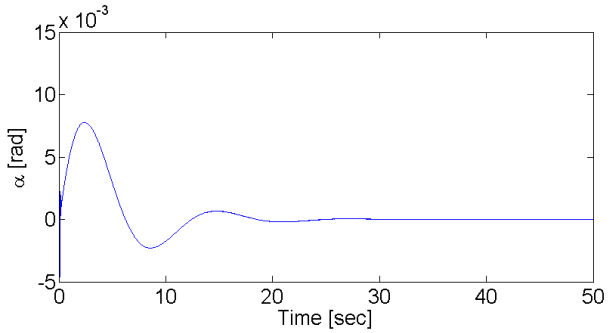

Fig. 3. Convergence for pitching, $\alpha(t)$ in $[rad]$.

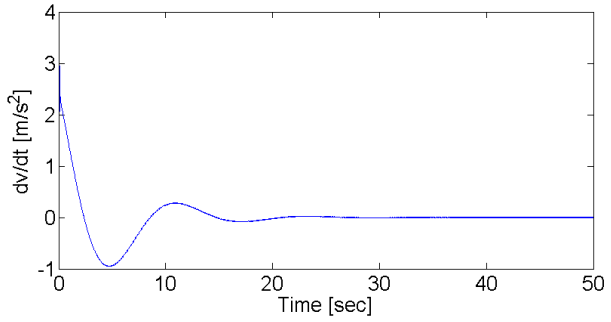

Fig. 4. Control input behavior, $\dot{v}_j(t)$ in $[\frac{m}{s^2}]$.

Milanese et al. (2008). These values are used in conjunction with the parameters I_1, I_2, and I_3 as described in (7) and (8). The control gains α_g, γ_1, γ_2 and k_s were manually selected as 2.5, 1, 1 and 1, respectively.

Fig. 2 shows the time evolution of $h(t)$, which demonstrates the rapid convergence of the system plunge to zero. Furthermore, Fig. 3 shows that the pitching displacement $\alpha(t)$ also converges to zero quickly. Fig. 4 shows the control effort $(\dot{v}_j(t))$ used during closed-loop controller operation. The commanded control input remains within reasonable limits throughout the duration of the simulation.

5. CONCLUSION

A nonlinear adaptive control law for LCO suppression in UAV wings is presented. The proposed control law is rigorously proven to achieve global asymptotic regulation of the plunging displacement to zero in the presence of dynamic model uncertainty and uncertain actuator dynamics. Furthermore, the proposed control law is shown via numerical simulation to simultaneously suppress the pitching displacement $\alpha(t)$. Future work will address LCO suppression control design, which can be proven to achieve simultaneous pitching and plunging regulation using only a scalar control input (i.e., the underactuated control problem).

ACKNOWLEDGEMENTS

The authors would like to thank the Air Force Research Laboratory Munitions Directorate and the American Society for Engineering Education for their support in this research.

REFERENCES

Amitay, M., Smith, D.R., Kibens, V., Parekh, D.E., and Glezer, A. (2001). Aerodynamic ow control over an unconventional airfoil using synthetic jet actuators. *AIAA Journal*, 39(3), 361–370.

Deb, D., Burkholder, J., and Smith, D. (2006). Adaptive synthetic jet actuator compensation for a nonlinear tailless aircraft model at low angles of attack. In *2006 American Control Conference*, 6. IEEE, Minneapolis, MN.

Deb, D., Tao, G., Burkholder, J.O., and Smith, D.R. (2005a). An adaptive inverse control scheme for synthetic jet actuator arrays. In *Infotech@Aerospace*.

Deb, D., Tao, G., Burkholder, J.O., and Smith, D.R. (2005b). An Adaptive Inverse Control Scheme for A Synthetic Jet Actuator Model. In *American Control Conference*, volume 82071, 2646–2651. IEEE, Portland, OR.

Deb, D., Tao, G., Burkholder, J.O., and Smith, D.R. (2007). Adaptive Compensation Control of Synthetic Jet Actuator Arrays for Airfoil Virtual Shaping. *Journal of Aircraft*, 44(2), 616–626.

Deb, D., Tao, G., Burkholder, J.O., and Smith, D.R. (2008). Adaptive Synthetic Jet Actuator Compensation for A Nonlinear Aircraft Model at Low Angles of Attack. *IEEE Transactions on Control Systems Technology*, 16(5), 983–995.

Dixon, W. (2007). Adaptive regulation of amplitude limited robot manipulators with uncertain kinematics and dynamics. *IEEE Transactions on Automatic Control*, 52(3), 488–493.

Dreyer, B. (2008). Simulation of Coupled Nonlinear Aeroelastic Response of an Airfoil Subject to A High-Intensity Gust. Technical Report May, Embry-Riddle Aeronautical University.

Frampton, K.D. and Clark, R.L. (2000). Experiments on control of limit cycle oscillations in a typical section. *Journal of Guidance, Control, and Dynamics*, 23, 956–960.

Jee, S.K., Lopez, O., Moser, R.D., Kutay, A.T., Muse, J.A., and Calise, A.J. (2009). Flow simulation of a

controlled airfoil with synthetic jet actuators. In *AIAA Conf. on Computational Fluid Dynamics*. San Antonio TX.

Jee, S., Lopez Mejia, O.D., Moser, R.D., Muse, J.A., Kutay, A.T., and Calise, A.J. (2013). Simulation of Rapidly Maneuvering Airfoils with Synthetic Jet Actuators. *AIAA Journal*, 51(8), 1883–1897.

Khalil, H.K. (2002). Simulation of Rapidly Maneuvering Airfoils with Synthetic Jet Actuators. In *American Control Conference*, volume 51. Prentice Hall, Upper Saddle River, NJ.

Liu, Y., Ciuryla, M., Amitay, M., Kwan, C., Myatt, J.H., Zhang, X., Ren, Z., and Casey, J.P. (2006). Integrated flight control and flow control using synthetic jet arrays. In *AIAA Guidance, Navigation, and Control Conference*. Keystone, CO.

Mackunis, W., Subramanian, S., Mehta, S., Ton, C., Curtis, J.W., and Reyhanoglu, M. (2013). Robust Nonlinear Aircraft Tracking Control Using Synthetic Jet Actuators. In *IEEE American Control Conference*, 1–8. IEEE, Eglin AFB, FL.

Milanese, A., De Breuker, R., Marzocca, P., and Abdalla, M. (2008). Distributed Synthetic Jet Actuators for the Control of Nonlinear Aeroelastic Systems. In *19th International Conference on Adaptive Structures and Technologies*, 1–12. ICAST, Minneapolis, MN.

Mondschein, S.T., Tao, G., and Burkholder, J.O. (2011). Adaptive actuator nonlinearity compensation and disturbance rejection with an aircraft application. In *American Control Conference*, 2951–2956.

O'Donnell, K.S., Marzocca, P., and Milanese, A. (2007). Design of a Wind Tunnel Apparatus to assist Flow and Aeroelastic Control via Zero Net Mass Flow Actuators. In *Structures, Structural Dynamics, and Materials Conference*, April, 1–12.

Platanitis, G. and Strganac, T.W. (2004). Control of a Nonlinear Wing Section Using Leading- and Trailing-Edge Surfaces. *Journal of Guidance, Control, and Dynamics*, 27(1), 52–58.

Rubillo, C., Bollt, E., and Marzocca, P. (2005). Active Aeroelastic Control of Lifting Surfaces via Jet Reaction Limiter Control. In *Structures, Structural Dynamics, and Materials Conference*, April, 18–21.

Satak, N., Hernandez, E.A.P., and Hurtado, J.E. (2012). Rate-free Control of Nonlinear Wing Section using Pitch and Plunge Measurements Only. In *AIAA Structures, Structural Dynamics and Materials Conference*, April, 1–7. AIAA, Honolulu, Hawaii.

Singhal, C., Tao, G., and Burkholder, J.O. (2009). Neural network-based compensation of synthetic jet actuator nonlinearities for aircraft flight control. In *AIAA Guidance, Navigation, and Control Conf.* Chicago, IL.

Strganac, T.W., K., J., and Thompson, D.E. (2000). Identification and control of limit cycle oscillations in aeroelastic systems. *Journal of Guidance, Control, and Dynamics*, 23, 1127–1133.

Tao, G. (1996). *Adaptive Control of Systems with Actuator and Sensor Nonlinearities*. John Wiley and Sons.

Tchieu, A.A., Kutay, A.T., Muse, J.A., Calise, A.J., and Leonard, A. (2008). Validation of a low-order model for closed-loop flow control enable flight. AIAA Paper 2008-3863.

Zergeroglu, A., Dixon, W., Behal, A., and Dawson, D. (2000). Adaptive set-point control of robotic manipulators with amplitude-limited control inputs. *Robotica*, 18(3), 71–181.